Pharmacological Research 121 (2017) 202–212

Contents lists available at ScienceDirect

Pharmacological Research

journal homepage: www.elsevier.com/locate/yphrs

Invited Review

ROS1 protein-tyrosine kinase inhibitors in the treatment of ROS1 fusion protein-driven non-small cell lung cancers

Robert Roskoski Jr.

Blue Ridge Institute for Medical Research, 3754 Brevard Road, Suite 116, Box 19, Horse Shoe, NC 28742-8814, United States

ARTICLE INFO

Article history:
Received 17 April 2017
Accepted 18 April 2017
Available online 30 April 2017

Chemical compounds studied in this article:
Cabozantinib (PubMED CID: 25102847)
Ceritinib (PubMED CID: 57379345)
Crizotinib (PubMED CID: 11626560)
Entrectinib (PubMED CID: 25141092)
Lorlatinib (PubMed CID: 71731823)

Keywords:
Acquired drug resistance
Catalytic spine
K/E/D/D
Protein kinase inhibitor classification
Protein kinase structure
Targeted cancer therapy

ABSTRACT

ROS1 protein-tyrosine kinase fusion proteins are expressed in 1–2% of non-small cell lung cancers. The ROS1 fusion partners include CD74, CCDC6, EZR, FIG, KDELR2, LRIG3, MSN, SDC4, SLC34A2, TMEM106B, TMP3, and TPD52L1. Physiological ROS1 is closely related to the ALK, LTK, and insulin receptor protein-tyrosine kinases. ROS1 is a so-called orphan receptor because the identity of its activating ligand, if any, is unknown. The receptor is expressed during development, but little is expressed in adults and its physiological function is unknown. The human *ROS1* gene encodes 2347 amino acid residues and ROS1 is the largest protein-tyrosine kinase receptor protein. Unlike the ALK fusion proteins that are activated by the dimerization induced by their amino-terminal portions, the amino-terminal domains of several of its fusion proteins including CD74 apparently lack the ability to induce dimerization so that the mechanism of constitutive protein kinase activation is unknown. Downstream signaling from the ROS1 fusion protein leads to the activation of the Ras/Raf/MEK/ERK1/2 cell proliferation module, the phosphatidyl inositol 3-kinase cell survival pathway, and the Vav3 cell migration pathway. Moreover, several of the ROS1 fusion proteins are implicated in the pathogenesis of a very small proportion of other cancers including glioblastoma, angiosarcoma, and cholangiocarcinoma as well as ovarian, gastric, and colorectal carcinomas. The occurrence of oncogenic ROS1 fusion proteins, particularly in non-small cell lung cancer, has fostered considerable interest in the development of ROS1 inhibitors. Although the percentage of lung cancers driven by ROS1 fusion proteins is low, owing to the large number of new cases of non-small cell lung cancer per year, the number of new cases of ROS1-positive lung cancers is significant and ranges from 2000 to 4000 per year in the United States and 10,000–15,000 worldwide. Crizotinib was the first inhibitor approved by the US Food and Drug Administration for the treatment of ROS1-positive non-small cell lung cancer in 2016. Other drugs that are in clinical trials for the treatment of these lung cancers include ceritinib, cabozantinib, entrectinib, and lorlatinib. Crizotinib forms a complex within the front cleft between the small and large lobes of an active ROS1 protein-kinase domain and it is classified as type I inhibitor.

Contents

Abbreviations: AS, activation segment; CS or C-spine, catalytic spine; CL, catalytic loop; EGFR, epidermal growth factor receptor; GK, gatekeeper; GRL, Gly-rich loop; InsR, insulin receptor; IRS2, insulin receptor substrate 2; JM, juxtamembrane segment; PKA, protein kinase A; ROS1$^+$ NSCLC, ROS1-positive non-small cell lung cancer; RS or R-spine, regulatory spine; Sh1, shell residue 1; TM, transmembrane.

E-mail address: rrj@brimr.org

http://dx.doi.org/10.1016/j.phrs.2017.04.022
1043-6618/

1. ROS1 fusion proteins and non-small cell lung cancers

ROS1 was discovered in the 1980s as the oncogene product of the chicken sarcoma RNA UR2 (University of Rochester) tumor virus [1–3]. After characterization of the viral oncogene and cellular proto-oncogene, the first full length sequence of the human ROS1 proto-oncogene, which was derived from a cDNA isolated from human glioblastoma cells, was reported by Birchmeier et al. in 1981 [4]. See Ref. [5] for a comprehensive review of the discovery of ROS1.

The *ROS1* gene encodes a receptor protein-tyrosine kinase that consists of 2347 amino acid residues making it the largest member of this enzyme-receptor family. ROS1 is related to ALK, LTK, and the insulin receptor families [6]. ROS1 contains a signal sequence of 27 amino acid residues, an extracellular domain of 1832 residues, a transmembrane segment of 23 residues, and an intracellular domain consisting of 465 residues. The intracellular domain contains a juxtamembrane segment (JM) of 62 residues, a protein kinase domain of 278 residues, and a C-terminal tail of 125 residues. The extracellular domain contains nine fibronectin III-like domains of about 90 amino acid residues each and three β-propellers of about 250 residues each that contain YWTD sequences (Fig. 1) [7–9]. *ROS1* knockout mice appear to be healthy except that males are infertile [10].

ROS1 is a so-called orphan receptor protein-tyrosine kinase because no activating ligand has (yet) been identified [5]. In part because of the absence of a known activating ligand, the physiological functions of ROS1 are unknown. This receptor is in various tissues and organs during embryonic development but with little expression in adults. Of some two dozen adult human tissues studied, the highest expression level (although slight) occurs in lung followed by cervix and colon. Oncogenic activation of ROS1 as a result of chromosomal rearrangements has been reported in patients with NSCLC (non-small cell lung cancer) [11–13], glioblastoma [14], cholangiocarcinoma [15], ovarian carcinoma [16], angiosarcoma [17], inflammatory myofibroblastic tumors [18], and Spitzoid melanocytic tumors [19].

The incidence of ROS1 fusion proteins in these neoplasms is generally quite low. The reported incidence of these fusion proteins in non-small cell lung cancer ranges from 1 to 2% [20]. Siegel et al. estimated that about 222,000 patients will develop lung cancer in the United States in 2017 (117,000 men and 105,000 women) and 156,000 people will die of the disease (85,000 men and 71,000 women) [21]. Assuming that 90% of these patients will have NSCLC, the incidence of new cases of *ROS1*$^{+}$ lung cancer will be about 2000–4000 (the incidence of chronic myelogenous leukemia will be about 9000 new cases in 2017). See Ref. [22] for an overview of the clinical course and treatment of small cell and non-small cell lung cancers.

Charest et al. reported that the amino-terminal portion of a protein called FIG (Fused in Glioblastoma) was fused to the carboxyterminal protein-tyrosine kinase domain of ROS1 in a human glioblastoma [14]. They found that an intra-chromosomal homozygous deletion of about 240 kilobases on 6q21 results in the formation of the FIG-ROS1 locus. The FIG-ROS1 fusion transcript is encoded by seven FIG exons and nine ROS1-derived exons. These investigators demonstrated that the FIG-ROS1 locus encodes an in-frame fusion protein with a constitutively active protein kinase activity and suggested that FIG-ROS1 may function as an oncogene. This was the first example of a fusion protein-tyrosine kinase that results from an intra-chromosomal deletion; other fusion proteins such as EML4-ALK result from the translocation between two chromosomes [22–24].

This FIG-ROS1 fusion protein occurs in NSCLC, cholangiocarcinoma, and ovarian cancer [25]. Other ROS1 fusion partners that have been reported in NSCLC include CD74, SDC4, SLC34A2, CCDC6, TMP3, LRIG3, and EZR (Fig. 2). The extracellular α-helical coiled-coil domains within CCDC66-ROS1, EZR-ROS1, FIG-ROS1, and TMP3-ROS1 may promote receptor dimerization and activation; otherwise, there is no indication of how activation of protein kinase activity of the other fusion proteins might occur. The CD74, EZR, and SLC34A2 fusion proteins occur with the greatest frequency in these lung cancers. The fusion proteins that begin with exon 32 contain a transmembrane segment that indicates that these isoforms contain an extracellular as well as an intracellular segment. Moreover, SLC34A2 and CD74 contain transmembrane segments so that the corresponding fusion proteins may be bi-membrane spanning proteins with an overall hairpin shape [5].

Owing to the lack of a known activating ligand, there have been few studies on the ROS1 signal transduction pathways [5]. The generation of chimeric receptors containing the extracellular domain of the epidermal growth factor or nerve growth factor receptors with the ROS1 protein kinase domain has been employed to study signaling pathways. These studies have coupled the chimeric receptors with protein kinase B (AKT), phosphatidyl inositol 3-kinase, STAT3, Vav3, the SH2 domain tyrosine phosphatases (SHP-1/2), and the mitogen-activated protein kinase ERK1/2. Many of these pathways are activated by other receptor protein-tyrosine kinases.

2. Properties of the ROS1 protein-tyrosine kinase domain

2.1. Primary, secondary, and tertiary structures of ROS1 and insulin receptor catalytic domains

The catalytic domain of ROS1 consists of 278 amino acid residues, which is an average size for a protein kinase. The stoichiometry of the ROS1 protein kinase reaction is given by the following chemical equation:

$$MgATP^{1-} + \text{protein-tyrosine} - O : H \rightarrow \text{protein-tyrosine} - O : PO_3{}^{2-} + MgADP + H^{+}$$

Note that the phosphorylium ion ($PO_3{}^{2-}$), but not the phosphate ($OPO_3{}^{2-}$) group, is transferred from ATP to the protein-tyrosine substrate.

Based upon the sequences of about five dozen protein-serine/threonine and protein-tyrosine kinases, Hanks and Hunter divided the primary structures into 12 domains (I-VIA, VIB-XI) [26]. Domain I of ROS1 contains a glycine-rich loop (GRL) with a GxGxΦG signature (^{1952}GSGAFG^{1957}), where Φ refers to a hydrophobic residue and is phenylalanine in the case of ROS1. The glycine-rich loop occurs between the β1- and β2-strands and overlays the ATP/ADP-binding site. Owing to its role in both ATP binding and ADP release, the glycine-rich loop must be flexible and protein

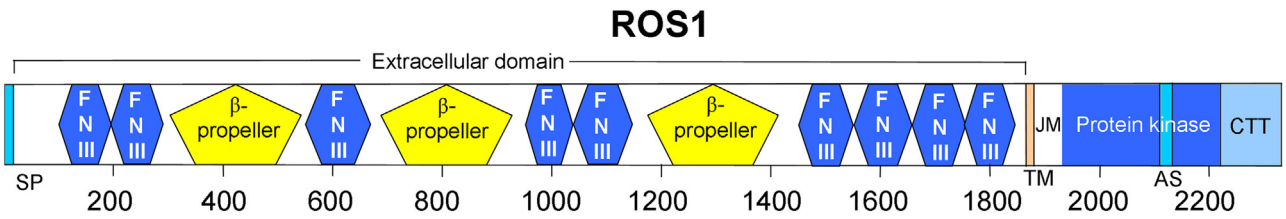

Fig. 1. The general structure of the ROS1 proto-oncogene. The amino acid residue numbers are given. AS, activation segment; CTT, C-terminal tail; FN III, fibronectin III-like domain; JM, juxtamembrane; SP, signal peptide; TM, transmembrane.

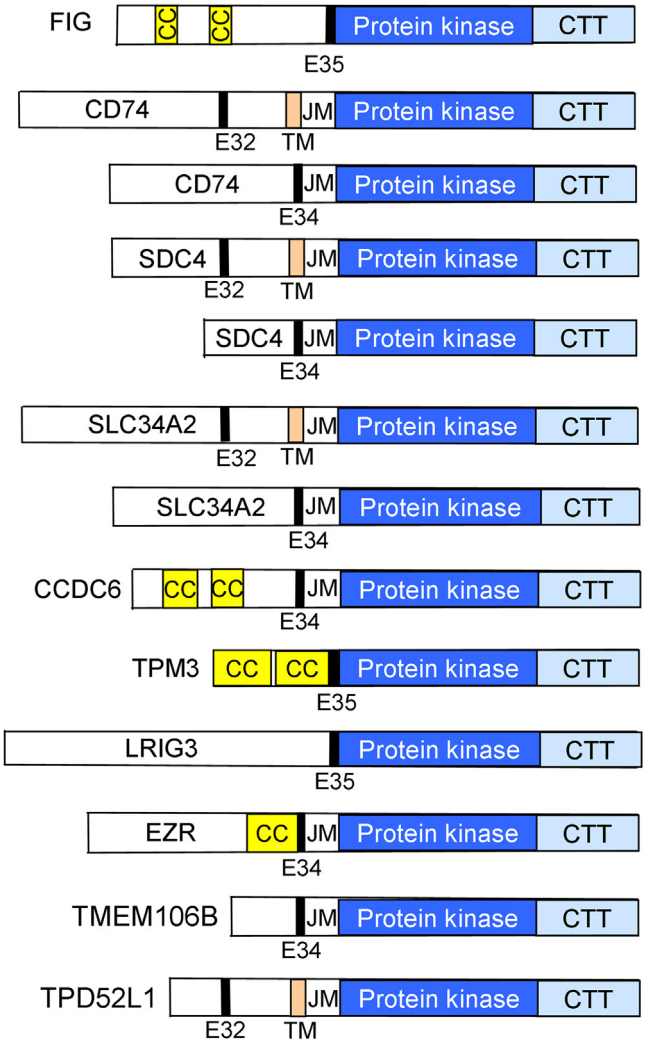

Fig. 2. Selected ROS1 fusion proteins that occur in NSCLC. FIG, fused in glioblastoma; CD74, cluster of differentiation 74; SDC4, syndecan 4; SLC34A2, solute carrier family 34 (sodium phosphate), member 2; CCDC6, coiled-coil domain-containing protein 6; TMP3, tropomyosin 3; LRIG3, leucine-rich repeats and immunoglobulin-like domains 3; EZR, ezrin; TMEM106B, transmembrane protein 106B; TPD52L1, tumor protein D53; CC, coiled-coil; CTT, carboxyterminal tail; E, ROS1 exon; JM, juxtamembrane; TM, transmembrane.

segments including glycine have this property. Domain II of ROS1 contains a conserved Ala-Xxx-Lys (^{1978}AVK^{1980}) sequence in the β3-strand and domain III contains a conserved glutamate (E1997) in the αC-helix that forms an electrostatic bond with the conserved β3-lysine in the active protein kinase conformation (Fig. 3A). Domain VIB of ROS1 contains a conserved HRD sequence, which forms part of the catalytic loop (^{2077}HRDLAARN^{2084}). Domain VII contains a ^{2102}DFG^{2104} signature and domain VIII contains a ^{2129}APE^{2131} sequence, which together represent the beginning and end of the ROS1 activation segment. The activation segment exhibits different conformations in the more active and less active protein kinase states. Protein kinase domains IX–XI make up the αE–αI helices.

The initial X-ray structure of the catalytic subunit of protein kinase A provided a valuable framework for understanding the interrelationship of the 12 domains and has enlightened our views on the fundamental biochemistry of the entire protein kinase

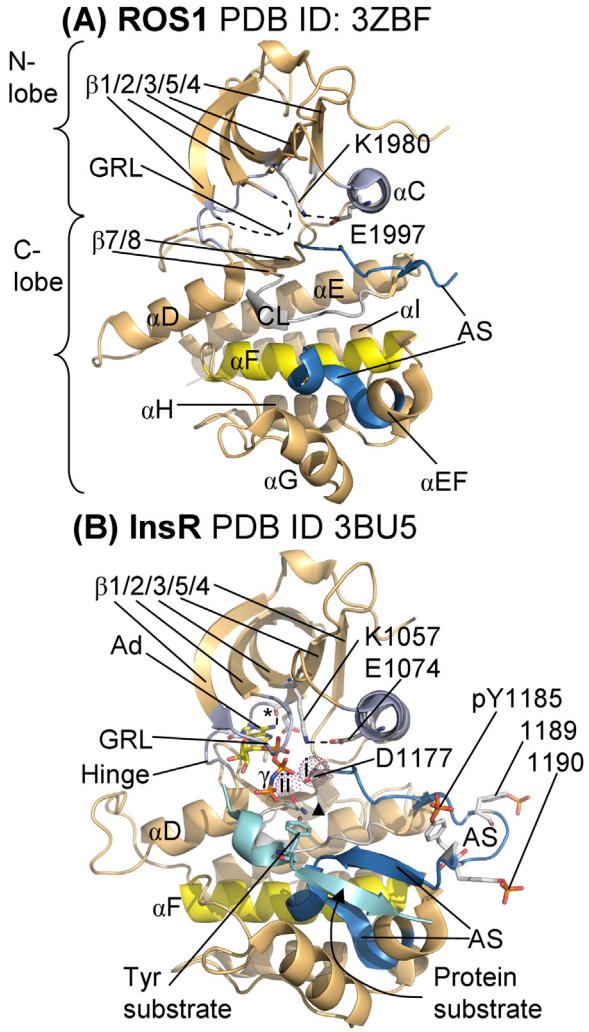

Fig. 3. (A) Structure of the ROS1 catalytic domain. The activation segment (AS) and the Gly-rich loop are not shown owing to their disorder; the inferred location of the Gly-rich loop (GRL) is indicated by the dashed curve. (B) Structure of the InsR catalytic domain together with a bound ATP and protein substrate. The dotted spheres represent the positions of Mg^{2+}(i) and (ii). The activation segment (blue) beginning with D1177 extends from the top to the bottom of the C-lobe and contains three phosphotyrosines (pY). Ad, adenine; *, E1104; ▲, N1164. Figs. 3–5, 7 and 8 were prepared using the PyMOL Molecular Graphics System Version 1.5.0.4 Schrödinger, LLC.

superfamily (PDB ID: 2CPK) [27,28]. All protein kinases including ROS1 have a small N-terminal and a large C-terminal lobe [29,30]. The small N-terminal lobe contains five conserved β-strands (β1–5) and an important regulatory αC-helix and the large C-terminal lobe contains four conserved short strands (β6–β9) along with seven helices (αD–αI and αEF) (Fig. 3A). Of the many hundreds of protein kinase structures that have been described, all of them possess the fundamental protein kinase structure as first described for the catalytic subunit of PKA [27,28,30].

All catalytically active protein kinases contain a K/E/D/D (Lys/Glu/Asp/Asp) signature that plays critical roles in the protein kinase reaction (Table 1) [30]. The lysine and glutamate occur within the N-terminal lobe and the two aspartate residues occur within the C-terminal lobe. Although ATP binds in a cleft between the two lobes, there is more extensive interaction with the N-terminal lobe. A salt bridge between the β3-lysine and the αC-glutamate is required for the formation of an active protein kinase, which corresponds to an αC_{in} configuration. These residues of many inactive enzyme conformations fail to make electrostatic contact and constitute an inactive αC_{out} structure (See Refs. [30,31] for details). The αC_{in} structure is necessary, but not sufficient, for the expression of catalytic activity.

The carboxyterminal lobe participates in protein/peptide substrate binding and contains catalytic loop residues that play an essential role in the phosphoryl transfer reaction. Moreover, two Mg^{2+} ions participate in each catalytic cycle of several protein kinases [32] and are most likely required for the functioning of ROS1. Of the two ROS1 X-ray structures in the public domain, neither contains ATP, a protein/peptide substrate, nor Mg^{2+}. Thus, we will use an active form of the related insulin receptor protein-tyrosine kinase (InsR) for comparative purposes. By inference, ROS1 D2102 (the DFG-D and the second D of K/E/D/D) binds to Mg^{2+}(i), which in turn binds to the β- and γ-phosphates of ATP. In this active conformation, the DFG-D is directed inward toward the active site. The corresponding residue in InsR is D1177 (Fig. 3B). ROS1 N2084 of the catalytic loop binds Mg^{2+}(ii), which in turn binds to the α- and γ-phosphates of ATP; the corresponding residue in InsR is N1164.

We infer that the activation segment of ROS1 in its active state forms an open structure that allows protein/peptide binding as depicted for the insulin receptor protein kinase domain complexed with a fragment of insulin receptor substrate 2 (IRS2) (Fig. 3B). The region of IRS2 that forms an antiparallel β-strand linkage with InsR is called the kinase regulatory loop binding (KRLB) region [33]. The carbonyl group of InsR G1167 within the activation segment forms a hydrogen bond with the N—H group of IRS2 I633 while the N—H group of G1167 hydrogen bonds with the carbonyl group of I633. Additionally, the carbonyl group of InsR G1169 within the activation segment forms a hydrogen bond with the N—H group of IRS2 I631 while the N—H group of G1169 forms a hydrogen bond with the carbonyl group of I631 (not shown). Knighton et al. reported that the N—H group of I22 of an inhibitory peptide substrate analogue forms a hydrogen bond with the carbonyl group with the activation segment PKA G200 [28]. The PKA inhibitor interaction involves I22, which is one residue downstream from the phosphorylation site (P + 1), while the IRS2 interactions are at the P + 3 and P + 5 positions. Both active and less active protein kinases contain an additional helix (αEF) near the end of the activation segment.

The exocyclic 6-amino nitrogen of ATP characteristically forms a hydrogen bond with the carbonyl backbone residue of the first ROS1 hinge residue (E2027) that connects the amino-terminal and carboxyterminal lobes of the protein kinase domain and the *N*1 nitrogen of the adenine base forms a second hydrogen bond with the N—H group of the third hinge residue (M2029, not shown). The 6-amino nitrogen of ATP forms an electrostatic bond with InsR E1104 (Fig. 3B). As noted later, most small-molecule steady-state ATP competitive inhibitors of protein kinases including ROS1 make hydrogen bonds with the backbone residues of the connecting hinge.

The activation segment binds the protein substrate thus playing an important role in the catalytic cycle [34]. The beginning of the segment is located near the N-terminus of the αC-helix and the conserved catalytic loop HRD. The interfaces of these units are linked by hydrophobic interactions. As in the case of most protein kinases [35], phosphorylation of a residue or residues within the activation segment converts a less-active to a more-active enzyme [36]. ROS1, InsR, IGF-1R (insulin-like growth factor 1 receptor), LTK (the closest relative of ROS1 [6]), IRRK (insulin receptor related kinase), and ROS1 contain three potential phosphorylatable tyrosine residues with a sequence YxxxYY. This segment is Y2110/Y2114/Y2115 in ROS1 (UniProtKB ID: P08922 numbering system) and Y1185/Y1189/Y1190 in InsR (UniProtKB ID: P06213). The following scheme describes the activation of InsR: phosphorylation of Y1189 is followed by that of Y1185 and then Y1190 [37]. This same ordering was found for IGF-1R with phosphorylation of the second tyrosine, followed by the first, and then by the third tyrosine in the YxxxYY sequence [38]. Whether this sequence of activation segment phosphorylation of ROS1 or the ROS1 fusion proteins occurs is unknown.

Lemmon and Schlessinger reviewed the mechanisms of activation of several receptor tyrosine-protein kinases and each of these mechanisms involves the ligand-induced formation of receptor dimers and subsequent protein kinase activation or it involves the ligand-induced activation of pre-formed dimers [9]. Following activation, one member of the dimer pair catalyzes the phosphorylation of activation segment tyrosine residues of the receptor partner along with the phosphorylation of other protein-tyrosines that creates docking sites for signal transduction proteins. Our knowledge of the mechanism of physiological ROS1 is nil owing to the lack of any known stimulating ligand. Although the amino-terminal segment of several ROS1 fusion proteins contains coiled-coil regions with a propensity to dimerize, several others lack such dimerization domains (Fig. 2). Thus, the mechanisms responsible for the activation of ROS1 and the ROS1 fusion proteins are currently unknown and represent a potentially fruitful area of investigation.

The catalytic loop surrounding the actual site of phosphoryl transfer within the large lobe consists of ^{2077}HRDLAARN^{2084} in ROS1. The catalytic aspartate (D2079) in ROS1, which is the first D of K/E/D/D, functions as a base that abstracts a proton from the protein-tyrosine substrate residue thereby facilitating its in-line nucleophilic attack onto the γ-phosphorus atom of ATP (Fig. 4) [39]. The catalytic segment AAR sequence occurs in many receptor protein-tyrosine kinases such as EGFR, platelet-derived growth factor receptor, and ROS1 while RAA occurs in many non-receptor protein-tyrosine kinases such as Src [26].

2.2. The hydrophobic spines of ROS1 and the insulin receptor catalytic domains

Kornev et al. analyzed the structures of 23 eukaryotic and prokaryotic protein kinases and they determined the role of several critical residues by a local spatial pattern alignment algorithm [40,41]. They classified eight hydrophobic residues as a catalytic or C-spine and four hydrophobic residues as a regulatory or R-spine. These spines contain amino acid residues from both the N-terminal and C-terminal lobes. The R-spine contains one residue from the regulatory αC-helix and another from the activation segment, both of which are major components that determine more active or less active enzyme states. The lower portion of the R-spine within the large lobe anchors the activation and catalytic loops in an active state and the C-spine tethers ATP within the interlobe cleft thus enabling catalysis. Moreover, the accurate alignment of both spines is necessary for the production of an active enzyme as described

Table 1
Important residues of the human ROS1, ALK, and insulin protein-tyrosine kinase receptors.[a]

	ROS1	ALK	InsR	Inferred function	Hanks no.
Swiss-Prot accession no.	P08922	Q9UM73	P06213		
No. of residues	2347	1620	1382		
Molecular Wt (kDa)[b]	263.9	176.4	156.3		
Signal sequence	1–27	1–18	1–27		
Extracellular domain	28–1859 FN-III, 101–196 FN-III, 197–285 β-propeller, 291–551 FN-III, 557–671 β-propeller, 684–934 FN-III, 947–1042 FN-III, 1043–1150 β-propeller, 1175–1425 FN-III, 1450–1556 FN-III, 1557–1656 FN-III, 1658–1751 FN-III, 1752–1854	19–1038 MAM1, 264–427 LDL-A, 437–473 MAM2, 478–636	28–956 FN-III, 624–726 FN-III, 757–842 FN-III, 853–947	Ligand binding	
Transmembrane segment	1860–1882	1039–1059	957–979	Links extracellular and intracellular domains and mediates dimer formation	
JM segment	1883–1944	1060–1115	980–1022	Potential regulatory role	
Protein kinase domain	1945–2222	1116–1392	1023–1298	Catalyzes transphosphorylation	
Glycine-rich loop	^{1952}GSGAFG^{1957}	^{1123}GHGAFG^{1128}	^{1030}GQGSFG^{1035}	Anchors ATP β-phosphate	I
β3-K of K/E/D/D	K1980	K1150	K1057	Forms salt bridges with ATP α- and β-phosphates	II
αC-E, E of K/E/D/D	E1997	E1167	E1074	Forms salt bridges with β3-K	III
Hinge residues	^{2027}ELMEGG^{2032}	^{1197}ELMAGG^{1202}	^{1104}ELMAHG^{1109}	Connects N- and C-lobes and hydrogen bonds with the ATP adenine	V
Catalytic loop, HRDLAARN	^{2077}HRDLAARN^{2084}	^{1047}HRDLAARN^{1054}	^{1157}HRDLAARN^{1164}	Plays both structural and catalytic functions	VIb
Catalytic loop HRD, First D of K/E/D/D	D2079	D1249	D1159	Catalytic base (abstracts protein substrate proton)	VIb
Catalytic loop Asn, HRDLAARN	N2084	N1254	N1164	Chelates Mg^{2+}(ii)	VIb
AS DFG, Second D of K/E/D/D	D2102	D1270	D1177	Chelates Mg^{2+}(i)	VII
AS	D2102–E2131	D1270–E1299	D1177–E1206	Positions protein substrate	VII–VIII
AS tyrosines	2110, 2114, 2115	1278,1282,1283	1185, 1189, 1190	Stabilizes the AS after phosphorylation	VIII
End of AS	^{2129}APE^{2131}	^{1297}PPE^{1299}	^{1204}APE^{1206}	Interacts with the αHI loop and stabilizes the AS	VIII
C-terminal tail	2223–2347	1393–1620	1299–1382	Signal transduction	None
C-terminal tail tyrosine phosphorylation sites	2274, 2334	1507, 1604	1355, 1361	Phosphorylated tyrosines interact with a variety of docking proteins that mediate intracellular signaling	None

[a] AS, activation segment; FN-III, fibronectin III-like domain; JM, juxtamembrane; LDL-A, low density lipoprotein class A domain; MAM, meprin-A5 antigen-PTPμ domain.
[b] Molecular weight of the unprocessed and nonglycosylated precursor.

for the cyclin-dependent protein kinases, EGFR, ERK1/2, the Janus kinases, MEK1/2, Src, and the vascular endothelial growth factor receptors [22,32,42–48].

Going from the base to the apex, the classical protein kinase regulatory spine consists of the catalytic loop HRD-His, the activation loop DFG-Phe, an amino acid four residues carboxyterminal to the conserved αC-glutamate, and an amino acid at the beginning of the β4-strand [40,41]. The backbone N—H of the HRD-His hydrogen bonds with an invariant aspartate carboxyl group within the very hydrophobic αF-helix. Going from the base to the apex of the spine, Meharena et al. dubbed the R-spine residues RS0, RS1, RS2, RS3, and RS4 (Fig. 4A) [49]. The R-spine of ROS1 is linear like that of the active InsR (Fig. 5B and C). The R-spine of inactive enzymes is usually nonlinear or broken, particularly involving the RS2 and RS3 residues (See Refs. [30,50] for details).

The catalytic spine of protein kinases contains residues from both the amino-terminal and carboxyterminal lobes; this spine is completed by the adenine base of ATP (Fig. 5A, C) [41]. The two residues of the small lobe that interact with the adenine base of ATP include a conserved valine residue at the beginning of the β2-strand (CS7) and a conserved alanine from the canonical AxK of the β3-strand (CS8). Furthermore, a hydrophobic residue from the β7-strand (CS6) interacts with the adenine portion of ATP. Almost all ATP-competitive protein kinase inhibitors interact with CS6. The CS6 residue occurs between two hydrophobic residues (CS4 and CS5) that contact the CS3 residue near the beginning of the αD-helix of the large lobe (Fig. 5A). CS4/6/5 immediately follow the catalytic loop asparagine (HRDxxxxN) so that it is easy to identify these residues based upon the primary structure. Finally, CS3 and CS4 make hydrophobic contacts with the CS1 and CS2 residues of the αF-helix thereby forming a completed catalytic spine (Fig. 4A and B) [41]. Significantly, the hydrophobic αF-helix, which spans the entire large lobe, anchors both spines. Moreover, both spines play an essential role in anchoring the protein kinase catalytic residues in an active conformation. CS7 and CS8 in the amino-terminal lobe make up the “ceiling” of the adenine-binding pocket while CS4/6/5 make up the “floor” of the binding pocket. Note that CS4/6/5 form the β7-strand of the protein kinase domain (Fig. 3A).

Based upon the results of site-directed mutagenesis studies, Meharena et al. identified three shell (Sh) residues in the catalytic

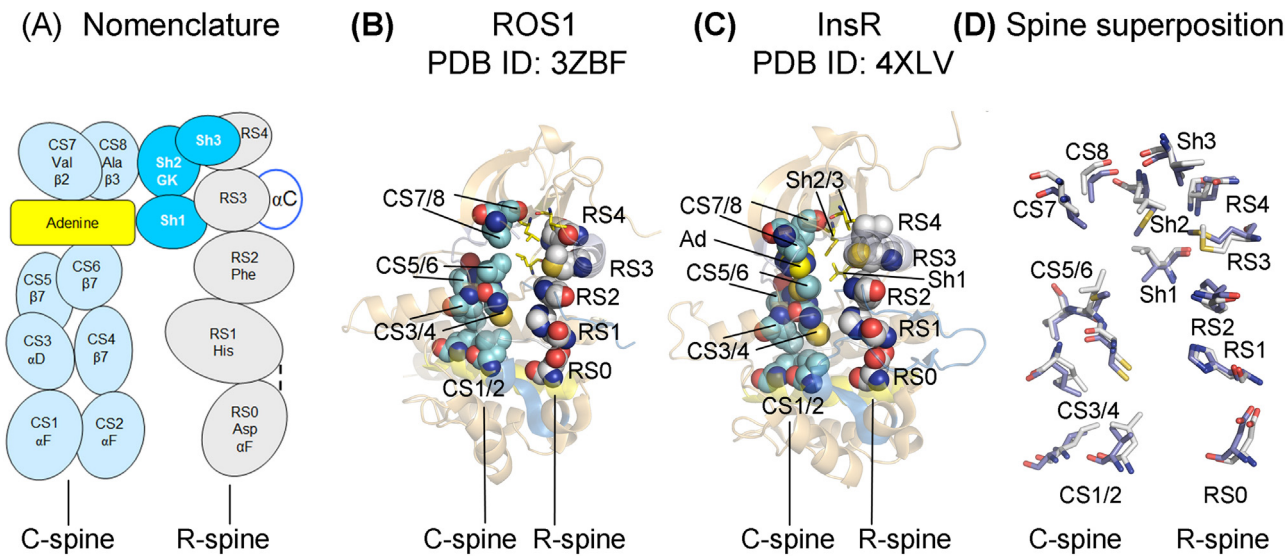

Fig. 5. Catalytic and regulatory spine structures. (A) Catalytic spine (CS), regulatory spine (RS), and shell (Sh) residues as observed from the classical frontal view of protein kinases. (B) Spines of active ROS1. (C) Spines of active InsR. (D) Superposition of the ROS1 and InsR spines. Ad, adenine.

Table 2
Spine and shell residues of human ROS1 and InsR and murine PKA.

	Symbol	KLIFS No.[a]	ROS1	InsRK	PKA[b]
Regulatory spine					
β4-strand (N-lobe)	RS4	38	Q2012	L1062	L106
C-helix (N-lobe)	RS3	28	M2001	M1051	L95
Activation loop F of DFG (C-lobe)	RS2	82	F2103	F1151	F185
Catalytic loop His/Tyr (C-lobe)	RS1	68	H2077	H1130	Y164
F-helix (C-lobe)	RS0	None	D2143	D1191	D220
R-shell					
Two residues upstream from the gatekeeper	Sh3	43	I2024	V1074	M118
Gatekeeper, end of β5-strand	Sh2	45	L2026	M1076	M120
αC-β4 loop	Sh1	36	L2010	V1060	V104
Catalytic spine					
β3-AxK motif (N-lobe)	CS8	15	A1978	A1028	A70
β2-strand (N-lobe)	CS7	11	V1959	V1010	V57
β7-strand (C-lobe)	CS6	77	L2086	M1139	L173
β7-strand (C-lobe)	CS5	78	V2087	V1140	I174
β7-strand (C-lobe)	CS4	76	C2085	C1138	L172
D-helix (C-lobe)	CS3	53	L2034	L1084	M128
F-helix (C-lobe)	CS2	None	I2150	V1198	L227
F-helix (C-lobe)	CS1	None	L2154	I1202	M231

[a] KLIFS (kinase–ligand interaction fingerprint and structure) from Ref. [54].
[b] From Refs. [40,41,49].

subunit of PKA that buttress and stabilize the regulatory spine, which they labeled Sh1, Sh2, and Sh3 [49]. The Sh2 residue corresponds to the gatekeeper residue. This designation indicates the role that the gatekeeper plays in controlling access to a back cleft or back pocket [51,52]; it is sometimes called hydrophobic pocket II (HPII) [52,53]. In contrast to the identification of the HRD, DFG, or APE signatures, which is based upon their primary structures [26], the spines were identified by their spatial locations in more active and less active protein kinases [40,41]. Table 2 provides a summary of the spine and shell residues of ROS1, InsR, and PKA. As described later, small molecule protein kinase antagonists often interact with residues that constitute the catalytic spine as well as regulatory spine and shell residues [50].

The ROS1 X-ray structures are those of an active protein kinase. For example, the DFG-Asp is pointed inward toward the active site, the configuration of the αC-helix is in its active αC_{in} configuration with E1997 forming a hydrogen bond with the β3-K1980, and the catalytic and regulatory spines are linear and are neither bent nor broken. Moreover the C- and R-spines are superimposable with the active, tris-phosphorylated form of InsR (Fig. 5D). However, it cannot be stated with certainty that ROS1 is active owing to the lack of the full structure of the activation segment. In the case of ALK (PDB ID: 2XP2), the spine residues were superimposable with the InsR, but the activation segment was closed and compact, a property of an inactive enzyme, which contrasts with the activation segments of active enzymes that are open and extended [22].

3. Drugs approved and in clinical trials for the treatment of ROS1$^+$ lung cancers

3.1. Clinical trials summary

Crizotinib is currently the only targeted drug that is approved for the treatment of ROS1$^+$ lung cancers (www.brimr.org/PKI/PKIs.htm). However, several additional drugs are in clinical trails for the treatment of these malignancies (Table 3). The code for the ROS1 inhibitors is useful in PubMed literature searches and PDB searches because it often results in findings that are missed when using the

Table 3
Properties of selected orally effective small molecule ROS1 inhibitors approved and in clinical trials.[a]

Name, code, trade name®	Targets	PubChem CID	Formula	MW (Da)	D/A[b]	cLogP[c]	FDA-approved indications[d]
Crizotinib, PF-2341066, Xalkori®	ALK, MET, LTK, ROS1	11626560	$C_{21}H_{22}Cl_2FN_5O$	450.3	2/6	3.7	ALK$^+$ (2011) and ROS1$^+$ NSCLC (2016)
Lorlatinib, PF-06463922	ALK, LTK, ROS1	71731823	$C_{21}H_{19}FN_6O_2$	406.4	1/7	1.5	None
Ceritinib, LDK 378, Zycadia®	ALK, IGF-1R, InsR, ROS1	57379345	$C_{28}H_{36}ClN_5O_3S$	558.1	3/8	6.4	ALK$^+$-NSCLC after crizotinib resistance (2014)
Entrectinib, RXDX-101	ALK, ROS1, Trk1/2/3	25141092	$C_{31}H_{34}F_2N_6O_2$	560.6	3/8	5.7	None
Cabozantinib, XL-184 and BMS-907351, Cometriq®	Axl, Flt-3, Kit, MET, ROS1, Tie-2, TrkB, VEGFR1/2/3	25102847	$C_{28}H_{24}FN_3O_5$	501.5	2/7	5.4	Medullary thyroid cancer (2012); renal cell carcinoma after one prior anti-angiogenic therapy (2016)

[a] clinicaltrials.gov.
[b] No. of hydrogen bond donors/acceptors.
[c] Calculated log of the partition coefficient as determined by MedChem Designer® v.1.0.1.15.
[d] www.brimr.org/PKI/PKIs.htm.

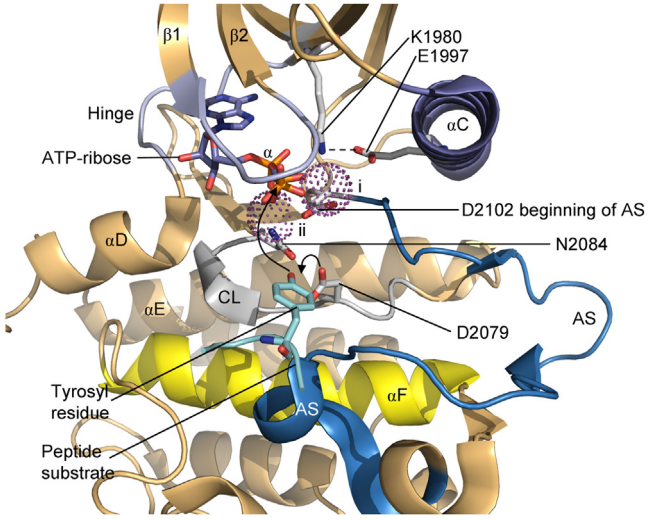

Fig. 4. Mechanism of the ROS1 protein kinase reaction. The catalytic loop D2079 functions as a base and abstracts a proton from the protein-tyrosine substrate. The dotted spheres represent Mg^{2+}(i) and Mg^{2+}(ii). AS, activation segment; CL, catalytic loop. The model is adopted from the fibroblast growth factor receptor-2 PDB ID: 2PVF, but the residue numbers correspond to ROS1.

generic or the trade name. See Ref. [55] for a summary of the clinical trials that led to the approval of crizotinib and for the status of the four other drugs that are included in this paper.

3.2. Structure of ROS1-drug complexes

The following provides an overview of drug-protein kinase interactions including ROS1. Drugs that are ATP-competitive inhibitors often bind to CS7 and CS8 within the small lobe and CS6 within the large lobe. These residues form hydrophobic contacts with the adenine base of ATP. Such drugs may form 1 to 3 hydrogen bonds with the backbone residues within the hinge. Many drugs interact with the gatekeeper residue by forming hydrogen bonds with the —R group or by making hydrophobic contact with the —R group. Because the ROS1 gatekeeper is leucine, interaction with the gatekeeper is expected to be hydrophobic in nature. Drugs frequently interact with residues within the αC-β4 back loop including the Sh1 residue. Many protein kinase antagonists bind to residues within the back pocket or back cleft that extends past the gatekeeper toward the αC-helix and toward the activation segment. The so-called selectivity pocket includes residues near the β5-strand and αC-helix within the back pocket, residues near the β3-lysine, αC-glutamate, and DFG-Asp, but it excludes residues that contact the adenine of ATP including CS6/7/8 [56]. Residues within the selectivity entrance include those at the end of the β1-strand just before the G-rich loop in the small lobe and those in the αD-helix within the large lobe; these residues form the mouth of the front pocket.

Crizotinib is the only FDA-approved small molecule inhibitor used in the treatment of metastatic ROS1$^+$ NSCLC (Table 3). The orally effective drug, which is an ATP-competitive inhibitor, contains a pyrazopyridine scaffold (Fig. 6A). The exocyclic 2-amino group of the pyridine ring forms a hydrogen bond with the carbonyl group of E2027 and the *N*1 of the pyridine ring forms a hydrogen bond with the N—H group of M2029 (Fig. 7A). This hydrogen bonding pattern mimics the bonding of the adenine base of ATP to the enzyme, *i.e.*, the exocyclic 6-amino group hydrogen bonds with the carbonyl group of the first residue of the hinge and the *N*1 of the adenine ring hydrogen bonds with the N—H group of the third residue of the hinge. Crizotinib makes hydrophobic contact with L1951 at the selectivity entrance before the G-rich loop, A1978 (CS8), L2010 in the αC-β4 back loop, L2026 (the Sh2 gatekeeper), L2086 (CS6), and DFG-D2102; the drug also makes van der Waals contact with R2083 and N2084 of the catalytic loop. The piperidine ring, which is attached to the pyrazol-4-yl moiety, is directed away from the enzyme into the solvent.

Crizotinib binds to active ROS1, which is a property of a type I inhibitor [50]. In contrast, the drug binds to inactive ALK (PDB ID: 2XP2) [22] with DFG-D_{in}. The drug binds to the front pocket, does not extend past the gatekeeper into the back pocket, and the crizotinib-ALK complex qualifies as a type 1 1/2B inhibitor [22,50]. The C-spine and R-spine residues of the crizotinib-ALK complex are superimposable with those of the active InsR, which suggests that the enzyme should be active. However, the activation segment of the ALK-drug complex is in an inactive conformation owing to the formation of an inhibitory αAS-helix at the beginning of the activation segment. Despite these differences, the hydrophobic interactions and the hydrogen bonding of crizotinib with the hinge residues of ALK corresponds to its interactions with ROS1.

To help in the classification of drug-kinase interactions, van Linden et al. have provided a comprehensive description of drug and ligand binding to more than 1200 human and mouse protein kinase domains [54]. Their KLIFS data base (kinase-ligand interaction

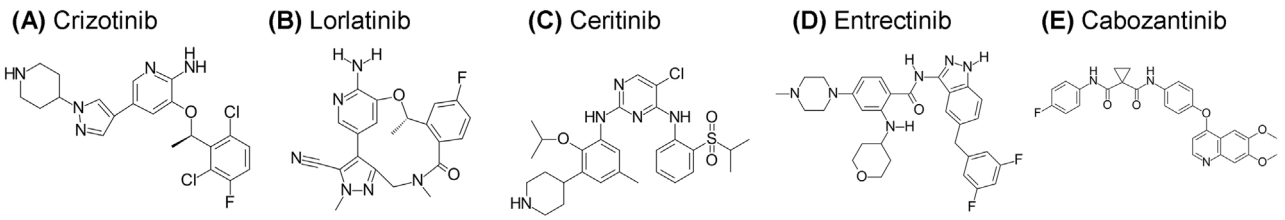

Fig. 6. Structures of selected ROS1 inhibitors.

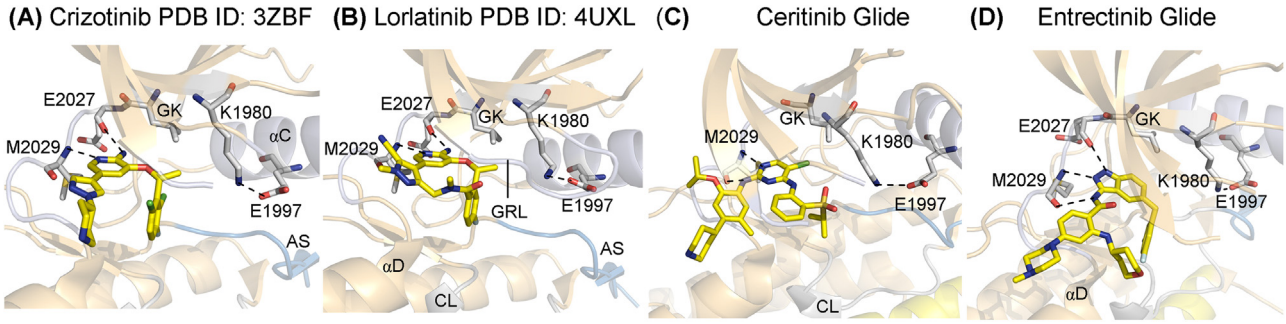

Fig. 7. Structures of ROS1-drug complexes. AS, activation segment; CL, catalytic loop; GK, gatekeeper; GRL, Gly-rich loop.

fingerprint and structure) describes the alignment of 85 protein kinase-ligand binding-site residues, which allows for the classification of ligands according to their binding properties along with the recognition of family-specific interaction features. Moreover, these investigators employ a standard residue numbering system that facilitates a comparison among all protein kinases. See Table 2 for the correspondence between the KLIFS residues and the R-spine, shell, and C-spine residues. Furthermore, van Linden et al. [54] have established an informative noncommercial and searchable web site that provides updated information on protein kinase-drug/ligand interactions (http://www.vu-compmedchem.nl/). The information provided at this site indicates that crizotinib binds to the ROS1 front pocket only.

Lorlatinib is an orally effective drug that is in clinical trails for the treatment of metastatic ROS1$^+$ NSCLC. The drug, which is an ATP-competitive inhibitor of ROS1, contains a pyrazopyridine scaffold similar to that of crizotinib (Fig. 6B). The exocyclic 2-amino group of the pyridine ring forms a hydrogen bond with the carbonyl group of E2027 and the *N*1 of the pyridine ring forms a hydrogen bond with the N—H group of M2029 (Fig. 7B). This hydrogen bonding is identical to that observed in the crizotinib-ROS1 complex. The drug makes hydrophobic contact with L1951 at the selectivity entrance before the G-rich loop, V1959 (CS7), A1978 (CS8), L2010 in the αC-β4 back loop, L2026 (the Sh2 gatekeeper), L2086 (CS6), and DFG-D2102; lorlatinib also makes van der Waals contact with R2083 and N2084 of the catalytic loop. The drug occupies the front pocket only and does not extend past the gatekeeper [54]. The nitrile group, which is attached to the pyrazol-4-yl moiety, is directed away from the enzyme into the solvent. Lorlatinib is a type I ROS1 inhibitor.

Ceritinib is a diamino-pyrimidine derivative (Fig. 6C) that is FDA approved for the treatment of ALK$^+$ NSCLC [57,58] and is in clinical trials for the treatment of ROS1$^+$ NSCLC (Table 3). No X-ray structural studies of ceritinib bound to ROS1 have been reported. To obtain an idea on the possible interaction of this drug with the enzyme, the Schrödinger Glide Suite (2016-1 release) was used to dock the drug into human ROS1 (with initially bound crizotinib, PDB ID: 3ZBF) [59]. The results indicate that the pyrimidine *N*1 forms a hydrogen bond with the N—H group of M2029 of the hinge residue while the exocyclic 2-amino group forms a hydrogen bond with the M2029 carbonyl function (Fig. 7C). The drug makes hydrophobic contact with V1959 (CS7), A1978 (CS8), L2019 within the αC-β4 back loop, L2026 (the Sh2 gatekeeper), L2028 within the hinge, T2036 within the αD-helix, L2086 (CS6), and DFG-D2102. The piperidinyl and isopropoxy groups are directed away from the protein kinase domain into the solvent. The interaction of ceritinib with ROS1 closely resembles that with ALK (PDB ID: 4MKC). However, the ALK activation segment is in an inactive configuration and the ceritinib-ALK complex is that of a type 1 1/2B inhibitor. In contrast, ceritinib binds to the active conformation of ROS1 and is therefore classified as a type I inhibitor [50].

Entrectinib is an indazole derivative (Fig. 6D) that is in clinical trials for the treatment of ROS1$^+$ NSCLC (Table 3). No X-ray structural studies of entrectinib bound to ROS1 have been reported. To explore the possible interaction of this drug with the enzyme, the Schrödinger Glide Suite (2016-1 release) was used to dock the drug into human ROS1 (with initially bound crizotinib, PDB ID: 3ZBF) [59]. The pose indicates that the indazole *N*1 functions as a hydrogen bond donor with the carbonyl group of E2027, the indazole *N*2 forms a hydrogen bond with the N—H group of M2029, and the indazole exocyclic 3-amino group forms a hydrogen bond with the carbonyl group of M2029 (Fig. 7D). Additional analysis indicates that the drug forms hydrophobic contacts with L1951 at the selectivity entrance before the G-rich loop, V1959 (CS7), A1979 (CS8), L2010 in the αC-β4 back loop, L2026 (the Sh2 gatekeeper), K2040 within the αD-helix, C2085 (CS4), L2086 (CS6), and DFG-D2102. Moreover, the drug makes van der Waals contact with R2083 and N2084 within the catalytic loop. The hydrophilic piperazine ring extends into the solvent. Like the three previous drugs, entrectinib is classified as a type I ROS1 inhibitor.

Cabozantinib is multi-kinase inhibitor that is FDA approved for the treatment of medullary thyroid cancer and renal cell carcinoma (Table 3). It is in clinical trials for the treatment of ROS1$^+$ NSCLC. Because no structural data of cabozantinib binding to ROS1 or any other protein kinase are in the public domain, we attempted to determine its mode of binding using *in silico* methodologies. Unfortunately, we were unable to obtain satisfactory poses using either the Schrödinger Glide or Induced Fit programs [59,60].

To summarize these interactions, the drugs form two or three hydrogen bonds with backbone residues within the hinge. Each of the drugs makes hydrophobic or van der Waals contact with an

Table 4
Crizotinib resistant ROS1 fusion-protein mutations in NSCLC.

Mutation[a]	Location	Mechanism of resistance
G2032R	Lower hinge	Most common mutation sterically blocks drug binding
D2033N	Lower hinge	Unclear
S1986Y/F	β3-αC loop	May sterically block drug binding
L2026M	Gatekeeper	Stabilizes the R-spine and increases enzyme activity
L2155S	End of αF-helix	Unclear

[a] From Ref. [55].

additional eight or nine residues. As described by Zhao et al. [56], interaction with CS7, CS8, and CS6 are among the most frequent ligand-protein kinase interactions. They also report that each ligand makes on the order of 14 contacts with its partner enzyme excluding hydrogen bonds. Our results are curated to include only the most significant interactions.

3.3. ROS1 resistance to crizotinib

Resistance to crizotinib can result from the activation of by-pass pathways, to mutations in the ROS1 protein kinase domain [55], or to as yet unidentified mechanisms. Activation of EGFR signaling was observed in the ROS1$^+$ HCC78 cell line that was derived from a human with NSCLC. Amplification of *KRAS* and an activating D618G Kit mutation have also been described. Five crizotinib resistance mutations in ROS1 have also been documented (Table 4). The G2032R and D2033N mutations occur in the hinge that connects the small and large lobes. Each of these mutations is close to the crizotinib-binding site and it is easy to imagine that the G2032R mutation with the substitution of the much larger arginine would block crizotinib binding. However, it is more difficult to imagine how the D2033N mutation would block drug binding because of their similar sizes. The S1986Y/F mutation occurs in the β3-αC loop; substitution of the much larger phenylalanine or tyrosine may sterically block crizotinib binding. The sizes of the leucine and methionine in the L2026M mutation are similar. However, studies in ALK indicate that a methionine gatekeeper may stabilize the R-spine to a greater extent than a leucine gatekeeper and this may account for enzyme activation and crizotinib resistance [22,23]. The L2155S mutation occurs at the end of the αF-helix and is about 23 Å from crizotinib; this distance suggests that this mutation results in structural changes of the protein kinase domain that render crizotinib ineffective (Fig. 8).

Ceritinib is a second generation drug that is effective in the treatment of ALK$^+$ crizotinib resistant mutations [22]; however, it does not appear to be as effective against the crizotinib resistant ROS1$^+$ tumors [55]. Lorlatinib appears to be effective against the ROS1 gatekeeper mutant and the D2033N and S1986Y/F mutants. Although entrectinib is effective against ROS1, it does not appear to be effective against the G2032R and L2026M mutations; it has not been tested with the other ROS1 mutants. Cabozantinib has been shown to be clinically effective in patients with the D2033N mutation; its effectiveness against the other mutations is not yet known. Owing to the relative paucity of ROS1$^+$ NSCLC patients and to the recent use of crizotinib in the treatment of these patients, all of the above data have been determined in very small numbers of subjects. Thus the data presented in this section are tentative in nature and future studies may lead to different conclusions.

4. Epilogue

Cui et al. initially developed crizotinib as a MET receptor protein-tyrosine kinase inhibitor [61]; MET is part of the insulin receptor family and is related to ALK and ROS1 [6]. In an informative paper,

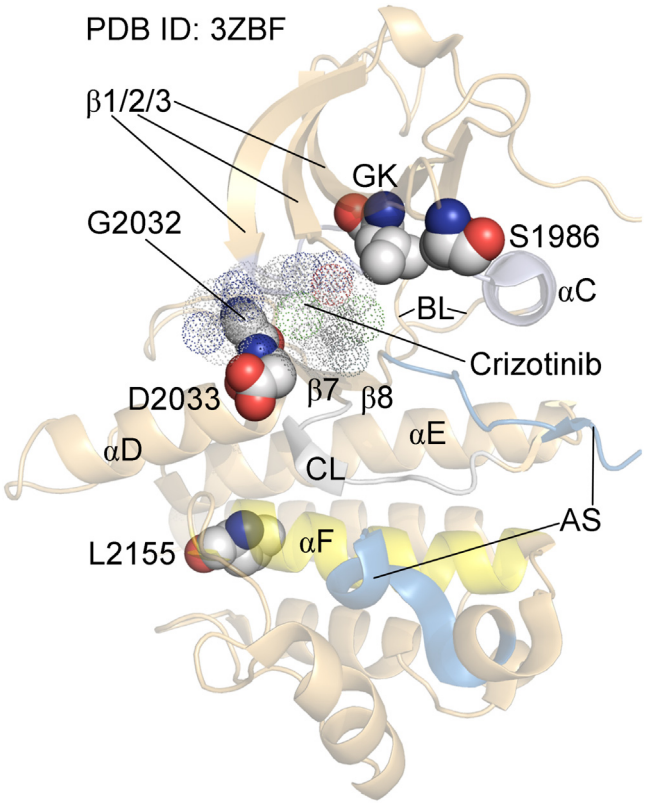

Fig. 8. The location of the crizotinib-resistant ROS1 mutations are shown as CPK spheres and crizotinib is depicted as dotted spheres. AS, activation segment; BL, αC-β4 back loop; CL, catalytic loop; GK, gatekeeper.

Cui et al. describe all of the steps in the development of crizotinib using structure-based drug design from a lead compound along with the use of lipophilic efficiency and ligand efficiency as developmental parameters [61]. Hepatocyte growth factor/scatter factor (HGF/SF) is the MET activating ligand and MET therefore corresponds to the hepatocyte growth factor receptor (HGFR). However, MET originally denoted the methyl group that occurs in the carcinogen (*N*-methyl-*N*′-nitroso-guanidine) used to generate a fusion protein in a human osteogenic sarcoma cell line [62]. Besides promoting cell division and survival, this protein kinase also plays a role in the metastasis of cancer cells. MET may also be thought of as an acronym for mesenchymal-epithelial transition factor [61]. During its development, crizotinib was also found to be an ALK inhibitor.

After the discovery that ROS1 fusion proteins participate in the pathogenesis of lung cancers, Lovly et al. reported that crizotinib inhibited ROS1 with an IC_{50} of 1.7 nM [63]. Subsequently, Mazières reported that crizotinib was highly effective in the treatment of patients with ROS1$^+$ lung cancers [64]. Owing to the clinical experience with crizotinib in the treatment of ALK$^+$ lung cancers, the transition to the treatment of patients with ROS1$^+$ lung cancers went easily. As noted above, primary and acquired resistance to crizotinib is a familiar problem associated with nearly all targeted cancer therapies.

As indicated in Table 3, all of the medicinals reviewed in this paper target several enzymes. The drug-enzyme structures of each of the four drugs depicted above indicate that they bind chiefly in the front pocket with little interaction with the selectivity pocket that extends from the front pocket (Fig. 7). Failure to interact with residues outside of the front pocket is consistent with the lack of selectivity of these drugs [56]. There are several hundred different small molecule protein kinase inhibitors in clinical trials world-

wide [58]. Although one goal in the development of protein kinase inhibitors has been to target a single enzyme, it seems that many, if not most, of the selective inhibitors have been found at later stages to inhibit multiple enzymes. Although it may be counterintuitive, the majority of the approved protein kinase antagonists are multikinase inhibitors (www.brimr.org/PKI/PKIs.htm). Moreover, their therapeutic success may be related to the simultaneous inhibition of multiple enzymes. Consequently, we have the issue of whether magic shotguns are to be favored over magic bullets [65].

Manning et al. found that the human protein kinase gene family consists of 518 members including 478 typical and 40 atypical enzymes [6]. Based upon the identity of the phosphorylated —OH group, these enzymes are classified as protein-tyrosine kinases (90), protein-tyrosine kinase like enzymes (43), and protein-serine/threonine kinases (385 members). A small group of proteins including MEK1/2, which catalyze the phosphorylation of both threonine and tyrosine residues within the activation segment of target proteins, are classified as dual specificity kinases. The protein-tyrosine kinases include both receptor (58) and non-receptor (32) proteins. Assuming a human gene number of 19,000 [66], protein kinases make up 2.7% of all genes. Accordingly, about one in 37 human genes on the average encodes a protein kinase. Because dysregulation and mutations of protein kinases play fundamental roles in the pathogenesis of human diseases including cancer, autoimmune, inflammatory, and nervous disorders, this family of enzymes has become one of the most important drug targets over the past two decades [67]. The three dozen FDA-approved drugs target only about 20 different protein kinases (www.brimr.org/PKI/PKIs.htm). Thus, there are still a very large number of additional potential targets that can be considered for the treatment of an increasing variety of diseases.

Conflicts of interest

The author is unaware of any affiliations, memberships, or financial holdings that might be perceived as affecting the objectivity of this review.

Acknowledgments

The colored figures in this paper were checked to ensure that their perception was accurately conveyed to colorblind readers [68]. The author thanks Laura M. Roskoski for providing editorial and bibliographic assistance. He also thanks Josie Rudnicki and Jasper Martinsek for their help in preparing the figures and Pasha Brezina and W.S. Sheppard for their help in structural analyses.

References

[1] P.C. Balduzzi, M.F. Notter, H.R. Morgan, M. Shibuya, Some biological properties of two new avian sarcoma viruses, J. Virol. 40 (1981) 268–275.
[2] M. Shibuya, H. Hanafusa, P.C. Balduzzi, Cellular sequences related to three new onc genes of avian sarcoma virus (*fps*, *yes*, and *ros*) and their expression in normal and transformed cells, J. Virol. 42 (1) (1982) 143–152.
[3] L.H. Wang, H. Hanafusa, M.F. Notter, P.C. Balduzzi, Genetic structure and transforming sequence of avian sarcoma virus UR2, J. Virol. 41 (1982) 833–841.
[4] C. Birchmeier, K. O'Neill, M. Riggs, M. Wigler, Characterization of ROS cDNA from a human glioblastoma cell line, Proc. Natl. Acad. Sci. U. S. A. 87 (1990) 4799–4803.
[5] J. Acquaviva, R. Wong, A. Charest, The multifaceted roles of the receptor tyrosine kinase ROS in development and cancer, Biochim. Biophys. Acta 1795 (2009) 37–52.
[6] G. Manning, D.B. Whyte, R. Martinez, T. Hunter, S. Sudarsanam, The protein kinase complement of the human genome, Science 298 (2002) 1912–1934.
[7] A.R. Kornblihtt, K. Umezawa, K. Vibe-Pedersen, F.E. Baralle, Primary structure of human fibronectin: differential splicing may generate at least 10 polypeptides from a single gene, EMBO J. 4 (1985) 1755–1759.
[8] T.A. Springer, An extracellular β-propeller module predicted in lipoprotein and scavenger receptors, tyrosine kinases, epidermal growth factor precursor, and extracellular matrix components, J. Mol. Biol. 283 (1998) 837–862.
[9] M.A. Lemmon, J. Schlessinger, Cell signaling by receptor tyrosine kinases, Cell 141 (2010) 1117–1134.
[10] E. Sonnenberg-Riethmacher, B. Walter, D. Riethmacher, S. Gödecke, C. Birchmeier, The c-*ros* tyrosine kinase receptor controls regionalization and differentiation of epithelial cells in the epididymis, Genes Dev. 10 (1996) 1184–1193.
[11] V.M. Rimkunas, K.E. Crosby, D. Li, Y. Hu, M.E. Kelly, T.L. Gu, et al., Analysis of receptor tyrosine kinase ROS1-positive tumors in non-small cell lung cancer: identification of a FIG-ROS1 fusion, Clin. Cancer Res. 18 (2012) 4449–4457.
[12] K. Takeuchi, M. Soda, Y. Togashi, R. Suzuki, S. Sakata, S. Hatano, et al., RET, ROS1 and ALK fusions in lung cancer, Nat. Med. 18 (2012) 378–381.
[13] Y. Suehara, M. Arcila, L. Wang, A. Hasanovic, D. Ang, T. Ito, et al., Identification of KIF5B-RET and GOPC-ROS1 fusions in lung adenocarcinomas through a comprehensive mRNA-based screen for tyrosine kinase fusions, Clin. Cancer Res. 18 (2012) 6599–6608.
[14] A. Charest, K. Lane, K. McMahon, J. Park, E. Preisinger, H. Conroy, et al., Fusion of FIG to the receptor tyrosine kinase ROS in a glioblastoma with an interstitial del(6)(q21q21), Genes Chromosom. Cancer 37 (2003) 58–71.
[15] T.L. Gu, X. Deng, F. Huang, M. Tucker, K. Crosby, V. Rimkunas, et al., Survey of tyrosine kinase signaling reveals ROS kinase fusions in human cholangiocarcinoma, PLoS One 6 (2011) e15640.
[16] A.H. Birch, S.L. Arcand, K.K. Oros, K. Rahimi, A.K. Watters, D. Provencher, et al., Chromosome 3 anomalies investigated by genome wide SNP analysis of benign, low malignant potential and low grade ovarian serous tumours, PLoS One 6 (2011) e28250.
[17] C.P. Giacomini, S. Sun, S. Varma, A.H. Shain, M.M. Giacomini, J. Balagtas, et al., Breakpoint analysis of transcriptional and genomic profiles uncovers novel gene fusions spanning multiple human cancer types, PLoS Genet. 9 (2013) e1003464.
[18] C.M. Lovly, A. Gupta, D. Lipson, G. Otto, T. Brennan, C.T. Chung, et al., Inflammatory myofibroblastic tumors harbor multiple potentially actionable kinase fusions, Cancer Discov. 4 (2014) 889–895.
[19] T. Wiesner, J. He, R. Yelensky, R. Esteve-Puig, T. Botton, I. Yeh, et al., Kinase fusions are frequent in Spitz tumours and spitzoid melanomas, Nat. Commun. 5 (2014) 3116.
[20] J.F. Gainor, A.T. Shaw, Novel targets in non-small cell lung cancer: ROS1 and RET fusions, Oncologist 18 (2013) 865–875.
[21] R.L. Siegel, K.D. Miller, A. Jemal, Cancer statistics, CA Cancer J. Clin. 67 (2017) 7–30.
[22] R. Roskoski Jr., Anaplastic lymphoma kinase (ALK) inhibitors in the treatment of ALK-driven lung cancers, Pharmacol. Res. 117 (2017) 343–356.
[23] R. Roskoski Jr., The preclinical profile of crizotinib for the treatment of non-small-cell lung cancer and other neoplastic disorders, Expert Opin. Drug Discov. 8 (2013) 1165–1179.
[24] R. Roskoski Jr., Anaplastic lymphoma kinase (ALK): structure, oncogenic activation, and pharmacological inhibition, Pharmacol. Res. 68 (2013) 68–94.
[25] H.Y. Zou, Q. Li, L.D. Engstrom, M. West, V. Appleman, K.A. Wong, et al., PF-06463922 is a potent and selective next-generation ROS1/ALK inhibitor capable of blocking crizotinib-resistant ROS1 mutations, Proc. Natl. Acad. Sci. U. S. A. 112 (2015) 3493–3498.
[26] S.K. Hanks, T. Hunter, Protein kinases 6. The eukaryotic protein kinase superfamily: kinase (catalytic) domain structure and classification, FASEB J. 9 (1995) 576–596.
[27] D.R. Knighton, J.H. Zheng, L.F. Ten Eyck, V.A. Ashford, N.H. Xuong, S.S. Taylor, et al., Crystal structure of the catalytic subunit of cyclic adenosine monophosphate-dependent protein kinase, Science 253 (1991) 407–414.
[28] D.R. Knighton, J.H. Zheng, L.F. Ten Eyck, N.H. Xuong, S.S. Taylor, J.M. Sowadski, Structure of a peptide inhibitor bound to the catalytic subunit of cyclic adenosine monophosphate-dependent protein kinase, Science 253 (1991) 414–420.
[29] S.S. Taylor, A.P. Kornev, Protein kinases: evolution of dynamic regulatory proteins, Trends Biochem. Sci. 36 (2011) 65–77.
[30] R. Roskoski Jr., A historical overview of protein kinases and their targeted small molecule inhibitors, Pharmacol. Res. 100 (2015) 1–23.
[31] D. Bajusz, G.G. Ferenczy, G.M. Keserű, Structure-based virtual screening approaches in kinase-directed drug discovery, Curr. Top. Med. Chem. (2017), http://dx.doi.org/10.2174/1568026617666170224121313.
[32] R. Roskoski Jr., Src protein-tyrosine kinase structure, mechanism, and small molecule inhibitors, Pharmacol. Res. 94 (2015) 9–25.
[33] J. Wu, Y.D. Tseng, C.F. Xu, T.A. Neubert, M.F. White, S.R. Hubbard, Structural and biochemical characterization of the KRLB region in insulin receptor substrate-2, Nat. Struct. Mol. Biol. 15 (2008) 251–258.
[34] S.S. Taylor, M.M. Keshwani, J.M. Steichen, A.P. Kornev, Evolution of the eukaryotic protein kinases as dynamic molecular switches, Philos. Trans. R. Soc. Lond. B Biol. Sci. 367 (2012) 2517–2528.
[35] B. Nolen, S. Taylor, G. Ghosh, Regulation of protein kinases; controlling activity through activation segment conformation, Mol. Cell 15 (2004) 661–675.
[36] D.J. Rawlings, A.M. Scharenberg, H. Park, M.I. Wahl, S. Lin, R.M. Kato, et al., Activation of BTK by a phosphorylation mechanism initiated by SRC family kinases, Science 271 (1996) 822–825.
[37] L. Wei, S.R. Hubbard, W.A. Hendrickson, L. Ellis, Expression, characterization, and crystallization of the catalytic core of the human insulin receptor protein-tyrosine kinase domain, J. Biol. Chem. 270 (1995) 8122–8139.
[38] S. Favelyukis, J.H. Till, S.R. Hubbard, W.T. Miller, Structure and autoregulation of the insulin-like growth factor 1 receptor kinase, Nat. Struct. Biol. 8 (2001) 1058–1063.

[39] J. Zhou, J.A. Adams, Participation of ADP dissociation in the rate-determining step in cAMP-dependent protein kinase, Biochemistry 36 (1997) 15733–15738.
[40] A.P. Kornev, N.M. Haste, S.S. Taylor, L.F. Ten Eyck, Surface comparison of active and inactive protein kinases identifies a conserved activation mechanism, Proc. Natl. Acad. Sci. U. S. A. 103 (2006) 17783–17788.
[41] A.P. Kornev, S.S. Taylor, L.F. Ten Eyck, A helix scaffold for the assembly of active protein kinases, Proc. Natl. Acad. Sci. U. S. A. 105 (2008) 14377–14382.
[42] R. Roskoski Jr., ErbB/HER protein-tyrosine kinases: structures and small molecule inhibitors, Pharmacol. Res. 79 (2014) 34–74.
[43] R. Roskoski Jr., Cyclin-dependent protein kinase inhibitors including palbociclib as anticancer drugs, Pharmacol. Res. 111 (2016) 784–803.
[44] R. Roskoski Jr., ERK1/2 MAP kinases: structure, function, and regulation, Pharmacol. Res. 66 (2012) 105–143.
[45] R. Roskoski Jr., Janus kinase (JAK) inhibitors in the treatment of inflammatory and neoplastic diseases, Pharmacol. Res. 111 (2016) 784–803.
[46] R. Roskoski Jr., MEK1/2 dual-specificity protein kinases: structure and regulation, Biochem. Biophys. Res. Commun. 417 (2012) 5–10.
[47] R. Roskoski Jr., Allosteric MEK1/2 inhibitors including cobimetanib and trametinib in the treatment of cutaneous melanomas, Pharmacol. Res. 117 (2017) 20–31.
[48] R. Roskoski Jr., Vascular endothelial growth factor (VEGF) and VEGF receptor inhibitors in the treatment of renal cell carcinomas, Pharmacol. Res. 120 (2017) 116–132.
[49] H.S. Meharena, P. Chang, M.M. Keshwani, K. Oruganty, A.K. Nene, N. Kannan, et al., Deciphering the structural basis of eukaryotic protein kinase regulation, PLoS Biol. 11 (2013) e1001680.
[50] R. Roskoski Jr., Classification of small molecule protein kinase inhibitors based upon the structures of their drug-enzyme complexes, Pharmacol. Res. 103 (2016) 26–48.
[51] K. Shah, Y. Liu, C. Deirmengian, K.M. Shokat, Engineering unnatural nucleotide specificity for Rous sarcoma virus tyrosine kinase to uniquely label its direct substrates, Proc. Natl. Acad. Sci. U. S. A. 94 (1997) 3565–3570.
[52] Y. Liu, K. Shah, F. Yang, L. Witucki, K.M. Shokat, A molecular gate which controls unnatural ATP analogue recognition by the tyrosine kinase v-Src, Bioorg. Med. Chem. 6 (1998) 1219–1226.
[53] J.J. Liao, Molecular recognition of protein kinase binding pockets for design of potent and selective kinase inhibitors, J. Med. Chem. 50 (2007) 409–424.
[54] O.P. van Linden, A.J. Kooistra, R. Leurs, I.J. de Esch, C. de Graaf, KLIFS: a knowledge-based structural database to navigate kinase-ligand interaction space, J. Med. Chem. 57 (2014) 249–277.
[55] F. Facchinetti, G. Rossi, E. Bria, J.C. Soria, B. Besse, R. Minari, et al., Oncogene addiction in non-small cell lung cancer: focus on ROS1 inhibition, Cancer Treat. Rev. 55 (2017) 83–95.
[56] Z. Zhao, L. Xie, L. Xie, P.E. Bourne, Delineation of polypharmacology across the human structural kinome using a functional site interaction fingerprint approach, J. Med. Chem. 59 (2016) 4326–4341.
[57] P. Wu, T.E. Nielsen, M.H. Clausen, FDA-approved small-molecule kinase inhibitors, Trends Pharmacol. Sci. 36 (2015) 422–439.
[58] P.M. Fischer, Approved and experimental small-molecule oncology kinase inhibitor drugs: a mid-2016 overview, Med. Res. Rev. 37 (2017) 314–367.
[59] R.A. Friesner, J.L. Banks, R.B. Murphy, T.A. Halgren, J.J. Klicic, D.T. Mainz, et al., Glide: a new approach for rapid, accurate docking and scoring. 1. Method and assessment of docking accuracy, J. Med. Chem. 47 (2004) 1739–1749.
[60] W. Sherman, T. Day, M.P. Jacobson, R.A. Friesner, R. Farid, Novel procedure for modeling ligand/receptor induced fit effects, J. Med. Chem. 49 (2006) 534–553.
[61] J.J. Cui, M. Tran-Dubé, H. Shen, M. Nambu, P.P. Kung, M. Pairish, et al., Structure based drug design of crizotinib (PF-02341066), a potent and selective dual inhibitor of mesenchymal-epithelial transition factor (c-MET) kinase and anaplastic lymphoma kinase (ALK), J. Med. Chem. 54 (2011) 6342–6363.
[62] L. Trusolino, A. Bertotti, P.M. Comoglio, MET signalling: principles and functions in development, organ regeneration and cancer, Nat. Rev. Mol. Cell Biol. 11 (2010) 843–848.
[63] C.M. Lovly, J.M. Heuckmann, E. de Stanchina, H. Chen, R.K. Thomas, C. Liang, et al., Insights into ALK-driven cancers revealed through development of novel ALK tyrosine kinase inhibitors, Cancer Res. 71 (2011) 4920–4931.
[64] J. Mazières, G. Zalcman, L. Crinò, P. Biondani, F. Barlesi, T. Filleron, et al., Crizotinib therapy for advanced lung adenocarcinoma and a ROS1 rearrangement: results from the EUROS1 cohort, J. Clin. Oncol. 33 (2015) 992–999.
[65] B.L. Roth, D.J. Sheffler, W.K. Kroeze, Magic shotguns versus magic bullets: selectively non-selective drugs for mood disorders and schizophrenia, Nat. Rev. Drug Discov. 3 (2004) 353–359.
[66] I. Ezkurdia, D. Juan, J.M. Rodriguez, A. Frankish, M. Diekhans, J. Harrow, et al., Multiple evidence strands suggest that there may be as few as 19, 000 human protein-coding genes, Hum. Mol. Genet. 23 (2014) 5866–5878.
[67] P. Cohen, D.R. Alessi, Kinase drug discovery–what's next in the field? ACS Chem. Biol. 8 (2013) 96–104.
[68] R. Roskoski Jr., Guidelines for preparing color figures for everyone including the colorblind, Pharmacol. Res. 119 (2017) 240–241.